© 2015. Published by The Company of Biologists Ltd | Development (2015) 142, 31-40 doi:10.1242/dev.111104

RESEARCH ARTICLE

STEM CELLS AND REGENERATION

Mga is essential for the survival of pluripotent cells during peri-implantation development

Andrew J. Washkowitz[1], Caroline Schall[1], Kun Zhang[2], Wolfgang Wurst[3,4], Thomas Floss[3], Jesse Mager[2] and Virginia E. Papaioannou[1,*]

ABSTRACT

The maintenance and control of pluripotency is of great interest in stem cell biology. The dual specificity T-box/basic-helix-loop-helix-zipper transcription factor Mga is expressed in the pluripotent cells of the inner cell mass (ICM) and epiblast of the peri-implantation mouse embryo, but its function has not been investigated previously. Here, we use a loss-of-function allele and RNA knockdown to demonstrate that *Mga* depletion leads to the death of proliferating pluripotent ICM cells *in vivo* and *in vitro*, and the death of embryonic stem cells (ESCs) *in vitro*. Additionally, quiescent pluripotent cells lacking *Mga* are lost during embryonic diapause. Expression of Odc1, the rate-limiting enzyme in the conversion of ornithine into putrescine in the synthesis of polyamines, is reduced in *Mga* mutant cells, and the survival of mutant ICM cells as well as ESCs is rescued in culture by the addition of exogenous putrescine. These results suggest a mechanism whereby *Mga* influences pluripotent cell survival through regulation of the polyamine pool in pluripotent cells of the embryo, whether they are in a proliferative or quiescent state.

KEY WORDS: Mga, Pluripotency, ESCs, T-box, Basic-helix-loop-helix-zipper, Transcription factor, Mouse, ODC

INTRODUCTION

By the time the mouse embryo implants in the uterus, three cell lineages have been established: first, the outer layer of trophectoderm (TE) separates from the inner cell mass (ICM), and then the ICM segregates into the inner pluripotent epiblast (EPI) and the primitive endoderm (PE), adjacent to the blastocoelic cavity. The PE and the TE undergo initial stages of differentiation through the actions of the transcription factor genes *Gata6* and *Cdx2*, respectively (Chazaud et al., 2006; Jedrusik et al., 2008; Johnson and McConnell, 2004; Silva et al., 2009; Strumpf et al., 2005), whereas the EPI remains pluripotent, largely through the action of the transcription factor genes *Pou5f1* (also known as *Oct4*), *Nanog* and *Sox2* (Avilion et al., 2003; Loh et al., 2006; Nichols et al., 1998; Silva et al., 2009). The maintenance of pluripotency in the ICM and EPI is essential for embryonic development, as the EPI will eventually differentiate into all of the tissues of the embryo.

The basic-helix-loop-helix-leucine-zipper (bHLHZip) domain genes of the MAX-interacting network are thought to play crucial roles in the development of the ICM and EPI (Grandori et al., 2000; Hurlin and Huang, 2006). This network of genes includes *Max* and *Mga*, as well as members of the Myc, Mad and Mnt families of transcription factors (Ayer et al., 1993; Hurlin et al., 1999, 1995; Meroni et al., 1997; Zervos et al., 1993). Only by forming heterodimers with MAX are MAX-network proteins able to bind DNA at the E-box sequence and to activate or repress transcription of E-box-containing target genes (Baudino and Cleveland, 2001; Hurlin et al., 1999; Meroni et al., 2000; Walker et al., 2005). Despite its near-universal expression in oocytes and throughout development, the role of zygotic MAX has been elucidated only in the peri-implantation period, in which it is essential for embryonic survival: embryos lacking *Max* die shortly after implantation, as maternal stores of MAX are depleted (Shen-Li et al., 2000). Embryos lacking Myc, Mnt and Mad family genes die after implantation. The binding partners of the MAX-network that are crucial for early development are unknown.

MGA, the least studied of the MAX-network transcription factors, is a dual-specificity transcription factor that contains both a bHLHZip domain and a T-box domain and is able to bind to and regulate transcriptional targets through both E-box sites as well as T-box-binding elements (TBEs). Heterodimerization with MAX is required for MGA to bind to E-box target gene promoters. On TBEs, MGA is able to bind alone, although activation or repression is modulated by heterodimerization with MAX (Hurlin et al., 1999).

In zebrafish, *Mga* mRNA was detected as a maternal transcript in the fertilized egg and is expressed widely throughout later development (Rikin and Evans, 2010). Morpholino depletion of *Mga* in fertilized zebrafish eggs results in defects in the brain, heart and gut derivatives, although no common transcriptional targets or pathways have been identified (Rikin and Evans, 2010). In mouse, *Mga* mRNA is first detected at E3.5 in the pluripotent ICM (Yoshikawa et al., 2006) and appears to be widely expressed during later organogenesis (Hurlin, et al., 1999). Expression of both mRNA and protein is seen in embryonic stem cells (ESCs), the *in vitro* analog of the ICM (Hu et al., 2009; van den Berg et al., 2010). In ESCs, MGA was found in a complex with POU5F1, and *Mga* knockdown leads to ESC differentiation, suggesting that MGA plays a role in the maintenance of pluripotency through its interaction with POU5F1 (Hammachi et al., 2012; Hu et al., 2009; van den Berg et al., 2010). To address the role of *Mga* in murine development, particularly its possible role in maintenance of pluripotency in the early embryo, we examined the development of mouse embryos lacking functional *Mga* through gene disruption and RNA knockdown.

RESULTS

Peri-implantation lethality of a loss-of-function *Mga* allele

A multipurpose, conditional *Mga* mutant allele, $Mga^{Gt(E153E01)Wrst}$, was generated by the German Gene Trap Consortium (Fig. 1). In its original orientation, here referred to as Mga^{Gt}, the endogenous

[1]Department of Genetics and Development, Columbia University Medical Center, New York, NY 10032, USA. [2]Department of Veterinary and Animal Science, University of Massachusetts, Amherst, Amherst, MA 01003, USA. [3]Institute of Developmental Genetics, Helmholtz Zentrum München – German Research Center for Environmental Health, Technical University of München, 85764 Neuherberg, Germany. [4]Deutsches Zentrum für Neurodegenerative Erkrankungen e. V. (DZNE), Standort München, and Munich Cluster for Systems Neurology (SyNergy), Adolf-Butenandt-Institut, Ludwig-Maximilians-Universität München, 80336 München, Germany.

*Author for correspondence (vep1@columbia.edu)

Received 8 April 2014; Accepted 9 November 2014

Development (2015) 142, 31-40 doi:10.1242/dev.111104

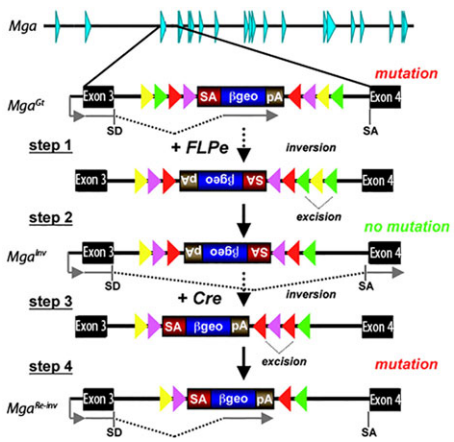

Fig. 1. The gene trap cassette and *Mga* mutations produced from the FlpRBG targeting vector. The Mga^{Gt} allele orients a splice acceptor-β-galactosidase-neomycin resistance cassette to accept the upstream exon 3 splice site of the *Mga* locus (top) and to create a mutant truncated reporter protein. After treatment with FLP recombinase (which results in inversion, step 1, and excision, step 2), the splice acceptor is no longer in the proper orientation to accept the upstream splice, and a wild-type transcript is produced by splicing around the inserted cassette. After further treatment with CRE recombinase, inversion and excision (steps 3 and 4) occur to produce the $Mga^{Re\text{-}inv}$ allele, which functions like the Mga^{Gt} allele producing a truncated reporter protein. Adapted from Schnutgen et al. (2005).

upstream exon donates a splice site that is accepted by the gene trap cassette, creating a truncated fusion protein that carries a *β-geo* reporter under the control of the *Mga* promoter. When exposed to FLPe recombinase, the cassette is inverted, a configuration referred to as Mga^{Inv}, and the splice acceptor is in the wrong orientation to accept the upstream splice, thus allowing the wild-type transcript to be produced. When subsequently exposed to CRE recombinase, the cassette is flipped once more, referred to as the $Mga^{Re\text{-}inv}$ configuration, producing the β-geo fusion protein. The Mga^{Gt} and $Mga^{Re\text{-}inv}$ alleles act as mutant reporter alleles and the Mga^{Inv} allele acts as a conditional-mutation allele (Fig. 1) (Schnutgen et al., 2005).

$Mga^{Gt/+}$ mice were recovered at the expected Mendelian frequency (42/88 from $Mga^{+/+}\times Mga^{Gt/+}$matings) and were viable and fertile. However, no $Mga^{Gt/Gt}$ mice were recovered at weaning from *inter se* matings of $Mga^{Gt/+}$ mice (0/84) (Table 1). $Mga^{Gt/+}$ mice were bred with a constitutively active FLPe recombinase-expressing mouse to generate the inverted conditional allele, Mga^{Inv} (Fig. 1). $Mga^{Inv/+}$ mice were born at the expected frequency (7/12 from $Mga^{+/+}\times Mga^{Inv/+}$ matings), indicating that the conditional $Mga^{Inv/+}$ allele did not have an obvious heterozygous or dominant negative effect (Table 1). Homozygous $Mga^{Inv/Inv}$ mice, however, were recovered at only ∼50% of the expected frequency (19/150 from $Mga^{Inv/+}\times Mga^{Inv/+}$ matings), indicating that the conditional Mga^{Inv} allele is not fully functional, although both male and female $Mga^{Inv/Inv}$ mice that were recovered had no apparent phenotype and were viable and fertile. This conditional allele was unable to compensate for the Mga^{Gt} mutation, as no $Mga^{Gt/Inv}$ mice were recovered at weaning (0/22 from $Mga^{Gt/+}\times Mga^{Inv/Inv}$ matings) (Table 1).

Dissection of the uteri of females from *inter se* $Mga^{Gt/+}$ matings at E9.5-E11.5 revealed only cellular debris or a few trophoblast giant cells in ∼1/4 of the deciduae (6/25). Trophoblast giant cells from one of these proved to be $Mga^{Gt/Gt}$ when genotyped by PCR (Table 2). Similarly, at E5.5, ∼1/4 of the deciduae were empty (9/44) and no homozygous mutants were recovered (Table 2). Histological examination at E5.5 and E6.5 showed instances of cellular debris with isolated trophoblast giant cells in ∼1/4 of deciduae (10/39 at E5.5; 4/10 at E6.5) (Fig. 2A). $Mga^{Gt/Gt}$ embryos were recovered from uterine flushes at a rate slightly lower than the expected Mendelian frequency at E4.5 (49/245) and at the expected frequency at E3.5 (21/89), and appeared morphologically normal (Table 2, Fig. 2A). Taken together, these results indicate that $Mga^{Gt/Gt}$ embryos develop to the blastocyst stage but die during the process of implantation.

Table 1. Number of progeny of each genotype recovered at weaning from the indicated matings

	Genotype			
Mating	+/+	+/–	–/–	*P*
$Mga^{+/+}\times Mga^{Gt/+}$	46	42	n.a.	n.s.
$Mga^{Gt/+}\times Mga^{Gt/+}$	31	53	0	*P*<0.0001
$Mga^{+/+}\times Mga^{Inv/+}$	5	7	n.a.	n.s.
$Mga^{Inv/+}\times Mga^{Inv/+}$	38	93	19	*P*=0.001
$Mga^{Gt/+}\times Mga^{Inv/Inv}$	N/A	22 *Inv*/+	0 *Gt*/*Inv*	*P*<0.0001

$Mga^{Gt/Gt}$ mice are not recovered indicating earlier lethality; $Mga^{Inv/Inv}$ mice are recovered at lower than Mendelian frequency and $Mga^{Gt/Inv}$ mice are not recovered, suggesting that Mga^{Inv} is a hypomorphic allele. n.a., not applicable; n.s., not significant.

Mga is expressed in the pluripotent ICM and EPI of the peri-implantation embryo

Embryonic expression of *Mga* was assessed using the Mga^{Gt} reporter allele. There was robust β-galactosidase activity in the EPI of $Mga^{Gt/+}$ embryos at E5.5 and E6.5, to the exclusion of the PE and extraembryonic tissues (Fig. 2B). Standard X-gal staining was insufficient for detection in preimplantation stages, but the more sensitive S-gal method showed staining in the EPI at E4.5 in $Mga^{Gt/+}$ embryos. Although neither X-gal nor S-gal showed staining at E3.5, RT-PCR for *Mga* in wild-type embryos demonstrated expression at E3.5 but not at E2.5 or E0.5 (one-cell stage) (Fig. 2B).

ICMs of blastocysts lacking *Mga* fail to thrive *in vitro*

Embryos were isolated at E3.5 from $Mga^{Gt/+}\times Mga^{Gt/+}$ matings, cultured *in vitro* for 4 days and then genotyped by PCR. Some cultures of $Mga^{Gt/+}$ embryos were stained with X-gal to assess β-galactosidase reporter activity. The ICM of the blastocyst cultures, but not the TE, showed strong X-gal staining after two days of culture, which later disappeared, indicating that embryonic expression of *Mga* was initially recapitulated in the *in vitro* culture system (data not shown). Whereas $Mga^{Gt/Gt}$ embryos (n=11) were able to attach to the tissue culture substrate and form a normal-appearing outgrowth of trophoblast giant cells, the ICM derivatives failed to thrive and did not form multicellular or cystic structures like their $Mga^{+/+}$ and $Mga^{Gt/+}$ littermates (n=35) (Fig. 3A). The outgrowth area of the ICM and TE was similar for wild-type and

Table 2. Number of embryos of each genotype recovered from $Mga^{Gt/+}\times Mga^{Gt/+}$matings at different developmental stages

	Genotype				
Stage	+/+	+/*Gt*	*Gt*/*Gt*	n.d.	*P*
E3.5	27	41	21	0	n.s.
E4.5	83	113	49	0	*P*=0.004
E5.5	12	23	0	9	*P*=0.003
E9.5-E11.5	6	13	1	5	*P*=0.04

$Mga^{Gt/Gt}$ embryos are present during preimplantation development (E3.5-E4.5) but are not recovered after implantation. n.d., not determined; n.s., not significant.

Development (2015) 142, 31-40 doi:10.1242/dev.111104

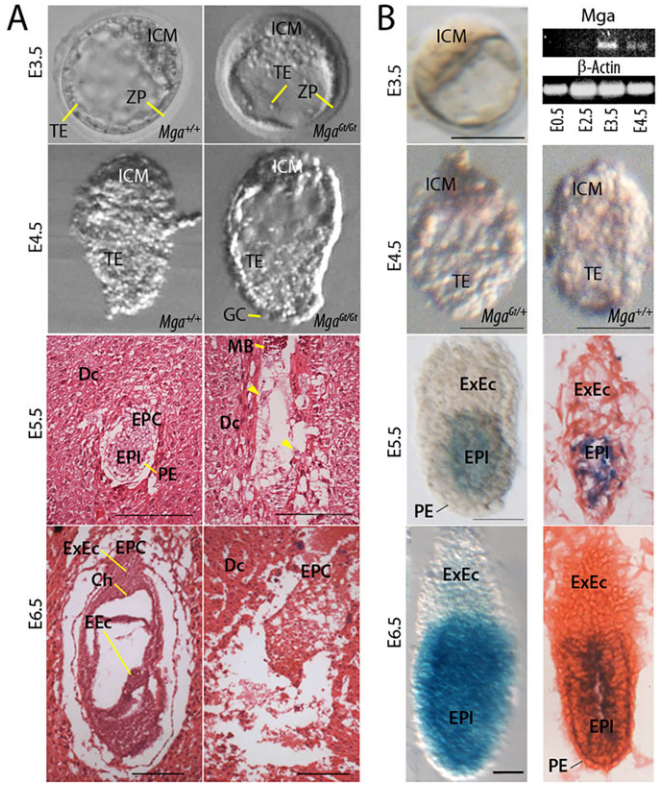

Fig. 2. *Mga* expression and *Mga*$^{Gt/Gt}$ embryos during peri-implantation development. (A) Development of *Mga*$^{Gt/Gt}$ embryos. Preimplantation embryos at E3.5 and E4.5 appear morphologically normal. In sections, embryo degeneration (right) was detected in 10/39 decidual swellings at E5.5 with some trophoblast giant cells (yellow arrowheads) and 4/10 swellings at E6.5. Other implantation sites contained morphologically normal embryos (left). (B) *Mga* expression in embryos using the β-galactosidase reporter and RT-PCR. No β-galactosidase activity was observed in blastocysts at E3.5 using X-gal staining. S-gal staining was present in the EPI of E4.5 *Mga*$^{Gt/+}$ embryos, but not of *Mga*$^{+/+}$ embryos. RT-PCR on pooled embryos did not detect any *Mga* transcripts at E0.5 or E2.5, but expression was present at E3.5 and E4.5 (top right). β-galactosidase staining was observed in the EPI of whole-mounts (on the left) and paraffin sections (on the right) at E5.5 and E6.5. MB, maternal blood; Dc, decidua; EPI. epiblast; EPC, ectoplacental cone; PE, primitive endoderm; ExEc, extraembryonic ectoderm; EEc, embryonic ectoderm; Ch, chorion; ICM, inner cell mass; TE, trophectoderm; ZP, zona pellucida; GC, giant cells. Scale bars: 100 µm.

mutant embryos after 2 days of culture, but by 4 days of culture the mutant ICMs had not increased in area, whereas the TE areas were similar to wild type (WT) (Fig. 3A). This indicates a failure of ICM survival as a contributing factor in the embryonic lethality of *Mga*$^{Gt/Gt}$ embryos. Culture of 41 blastocysts from heterozygous crosses that were allowed to attach and were then cultured in 2i medium for two additional days resulted in 9 (22%) outgrowths with little or no ICM. This matched closely the expected number of homozygous mutants (χ^2=0.20, P>0.1), indicating that 2i medium was insufficient to overcome the deficiency of Mga.

We also generated blastocysts lacking *Mga* through RNAi by microinjection of long double-stranded RNA into zygotes, an approach that has been used to elicit gene-specific knockdown (Wianny and Zernicka-Goetz, 2000; Zhang et al., 2012b). Most embryos injected with dsGfp as a control hatched from the zona pellucida (77%; 23/30), and showed robust TE and ICM outgrowth *in vitro* (60%; 18/30) (Fig. 4A,B). By contrast, only 42% (11/26) of dsMga-injected blastocysts hatched, and whereas most showed evidence of TE cells, only 4% (1/26) had a morphologically evident ICM after 3 days of culture (Fig. 4A,C). These results indicate that dsMga embryos precisely phenocopy *Mga*$^{Gt/Gt}$ embryos, and they strongly support that *Mga*^{Gt} is a null allele.

ESCs lacking *Mga* have a growth defect

Failure of *in vitro* ICM growth from *Mga*$^{Gt/Gt}$ embryos precluded establishment of mutant ESCs and suggested that ESCs would fail to thrive in the absence of *Mga*. To test this hypothesis, we derived ESCs in serum-containing medium (mES) from embryos homozygous for the conditional allele *Mga*^{Inv} that also carried the tamoxifen-inducible, ubiquitously expressed *ROSA26*$^{cre\text{-}ERT2}$ allele (de Luca et al., 2005), hereafter referred to as *creERT2*. *Mga*$^{Inv/Inv}$*; creERT2* ESCs were morphologically indistinguishable from *Mga*$^{Inv/+}$ ESCs, grew at similar rates and expressed pluripotency markers POU5F1 (OCT4) and NANOG (data not shown). Upon the addition of 4-hydroxytamoxifen to the culture media, however, there appeared to be a large amount of cell death, and surviving colonies of *Mga*$^{Inv/Inv}$*; creERT2* cells, which were normal in appearance (Fig. 3B), were smaller and sparser than *Mga*$^{Inv/Inv}$*; creERT2* cells without 4-hydroxytamoxifen or *Mga*$^{Inv/+}$ cells with or without 4-hydroxytamoxifen. Quantification of cell number at 24-h intervals revealed a ∼35% decrease in the number of cells in *Mga*$^{Inv/Inv}$*; creERT2* cultures with 4-hydroxytamoxifen compared with the controls (Fig. 3B). Genotyping of the surviving colonies revealed that there was incomplete CRE-induced inversion of the *Mga*^{Inv} allele regardless of the length of 4-hydroxytamoxifen treatment (Fig. 3B). Increasing the concentration of 4-hydroxytamoxifen beyond 0.5 µM resulted in toxicity for both *Mga*$^{Inv/Inv}$*; creERT2* and *Mga*$^{Inv/+}$ cells, but the amount of inversion of the *Mga*^{Inv} allele remained constant (data not shown). Together, these results indicate that in 4-hydroxytamoxifen-treated cultures, the surviving colonies had escaped complete inversion and that at least one functional *Mga* allele is necessary for the survival of ESCs.

Embryos lacking *Mga* have increased apoptosis

Reduced ICM outgrowth of *Mga*$^{Gt/Gt}$ blastocyst cultures and reduced growth of 4-hydroxytamoxifen-treated *Mga*$^{Inv/Inv}$*; creERT2* ESCs suggests an increase in cell death and/or a decrease in cell proliferation in the ICM or ICM derivatives in the absence of *Mga*. Counts of phosphorylated histone H3 (phospho-H3)-positive cells in the EPI did not reveal any difference in the number of mitotic cells in *Mga*$^{Gt/Gt}$ embryos (3.1±0.8) compared with *Mga*$^{+/+}$ and *Mga*$^{Gt/+}$ embryos (2.8±0.3) at E4.5 (t=0.259, P=0.65) (Fig. 5). The number of cells in prophase in *Mga*$^{Gt/Gt}$ embryos (1.6±0.5), indicated by uniform nuclear phospho-H3 staining, was similar to that in *Mga*$^{+/+}$ and *Mga*$^{Gt/+}$ embryos (1.8±0.3). Likewise, the number of cells in metaphase or anaphase in *Mga*$^{Gt/Gt}$ embryos (1.5±0.6), indicated by punctate staining indicative of condensed chromatin (Brenner et al., 2003), was similar to that in *Mga*$^{+/+}$ and *Mga*$^{Gt/+}$ embryos (1.0±0.2). Together, these data indicate that there is no defect in progression through the cell cycle in *Mga*$^{Gt/Gt}$ embryos.

To investigate apoptosis, immunofluorescence of E4.5 day embryos with antibodies against cleaved caspase 9 was performed (Zhu et al., 2012). A greater proportion of *Mga*$^{Gt/Gt}$ embryos (7/9) had cleaved caspase 9-positive fragmented nuclei than did *Mga*$^{+/+}$ and *Mga*$^{Gt/+}$ littermates (7/47) (P=0.012; Fisher's Exact Probability test) (Fig. 5). There was no difference in the proportion of *Mga*$^{+/+}$ embryos with cleaved caspase 9-positive fragmented nuclei (3/20) compared with *Mga*$^{Gt/+}$ embryos (4/27) (P=1.00; Fisher's Exact Probability test). These findings support the lack of a heterozygous phenotype and indicate that cell death as opposed to defective cellular proliferation is the cause of the embryo lethality.

Development (2015) 142, 31-40 doi:10.1242/dev.111104

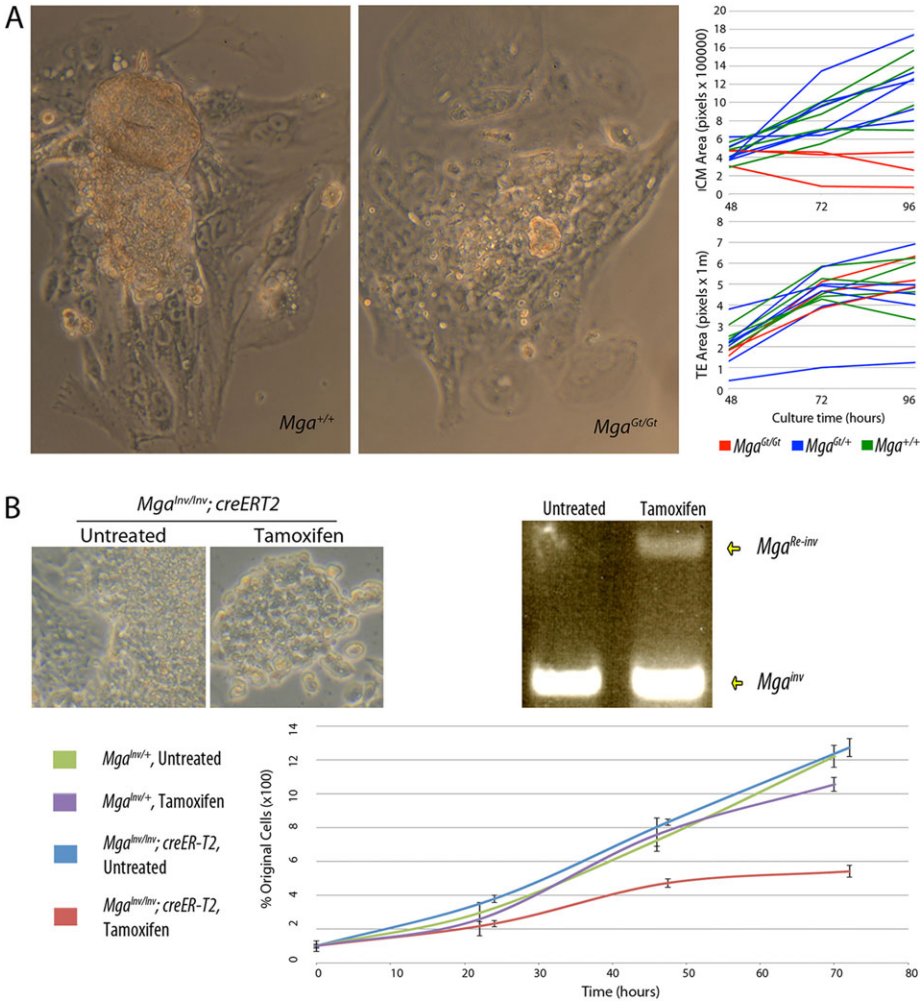

Fig. 3. *In vitro* culture shows defective growth of *Mga* mutant cells. (A) ICM outgrowth from $Mga^{Gt/Gt}$ embryos was severely compromised by 4 days of culture compared with WT, as seen by phase contrast microscopy. Measurement of the surface area on individual embryos at daily intervals showed that the ICM of $Mga^{Gt/Gt}$ embryos failed to grow (top right), although the increase in TE outgrowth was similar (bottom right). (B) ESC colonies appeared morphologically normal when inversion was induced with tamoxifen (middle), although inversion was incomplete as measured by PCR (right). $Mga^{Inv/Inv}$; *creERT2* ESCs grew at a slower rate from the time of addition of tamoxifen at t=0 (bottom).

Early differentiation of the ICM is not affected by the absence of *Mga*

At E4.5, the pluripotent ICM differentiates into two cell layers: the EPI, which remains pluripotent, and the PE, which forms an epithelial sheet at the blastocoel surface. Immunofluorescence with antibodies against the pluripotency marker NANOG, which marks the EPI, and GATA4, which marks the PE, showed that both layers form normally in $Mga^{Gt/Gt}$ embryos at E4.5 (n=3) (Fig. 5). To assess expression of the pluripotency marker *Pou5f1*, a *Pou5f1* GFP reporter allele, $Pou5f1^{tm2Jae}$ (Lengner et al., 2007), was bred into the Mga^{Gt} background. Immunofluorescence with anti-GFP antibodies showed a compacted EPI in $Mga^{+/+}$ and $Mga^{Gt/+}$ (n=27) as well as $Mga^{Gt/Gt}$ (n=7) embryos (Fig. 5). Together, these results indicate that $Mga^{Gt/Gt}$ embryos show the normal spatial and temporal gene expression pattern characteristic of the differentiation of PE and maintenance of pluripotency in the EPI.

Embryos lacking *Mga* lose pluripotent cells during diapause

Despite the presence of pluripotency markers at E4.5, the death of ICM derivatives *in vivo* and *in vitro* suggests that pluripotent cell maintenance is affected in $Mga^{Gt/Gt}$ embryos. To test this, we examined embryos in which diapause or implantation delay was induced by tamoxifen and depot medroxyprogesterone 17-acetate (DMPA) injections at E2.5 (Nichols et al., 2001). In diapause, the EPI and PE layers form but cell division ceases. RT-PCR of pooled wild-type embryos shows that one day after induction of diapause, *Mga* expression is at a level similar to E3.5 embryos and then falls to a low level at 4 and 7 days of diapause (Fig. 6C, and data not shown). Immunofluorescence using antibodies against NANOG and GATA4 was used to assess the persistence of EPI and PE cell populations, respectively, throughout diapause. One day after induction of diapause, $Mga^{Gt/Gt}$ embryos showed similar expression patterns of NANOG and GATA4 and a similar number of NANOG-expressing cells (16.5±1.5) compared with $Mga^{+/+}$ and $Mga^{Gt/+}$ controls (13.7±1.2) (z=1.17, P=0.24; Mann–Whitney U-test) (Fig. 6A). However, by 4 days after diapause induction, there were fewer NANOG-expressing cells in $Mga^{Gt/Gt}$ embryos (5.4±1.0) compared with controls (18.1±0.9) (z=3.240, P=0.001), although the relative position and number of GATA4-expressing cells was similar in $Mga^{Gt/Gt}$ (21.9±2.8) compared with controls (26.6±1.3) (z=0.98, P=0.33) (Fig. 6B). By 7 days after diapause induction, there were virtually no NANOG-positive cells in $Mga^{Gt/Gt}$ embryos (0.3±0.3), whereas in $Mga^{+/+}$ and $Mga^{Gt/+}$ embryos, NANOG-positive cells persisted (12.5±1.4) (z=2.39, P=0.02). In contrast to earlier time points, the number of GATA4-positive cells was also reduced in $Mga^{Gt/Gt}$ embryos (6.7±0.9) compared with controls (35.7±2.4) (z=2.39, P=0.02) (Fig. 6B). As has been observed in diapause embryos deficient for *Nanog* (Silva et al., 2009), GATA4-positive cells appeared flattened against the TE. Whereas formation of embryonic cell layers occurs normally, the declining number of NANOG-positive EPI cells in $Mga^{Gt/Gt}$ embryos during diapause implies that the pluripotent cells of the EPI are not maintained without

Development (2015) 142, 31-40 doi:10.1242/dev.111104

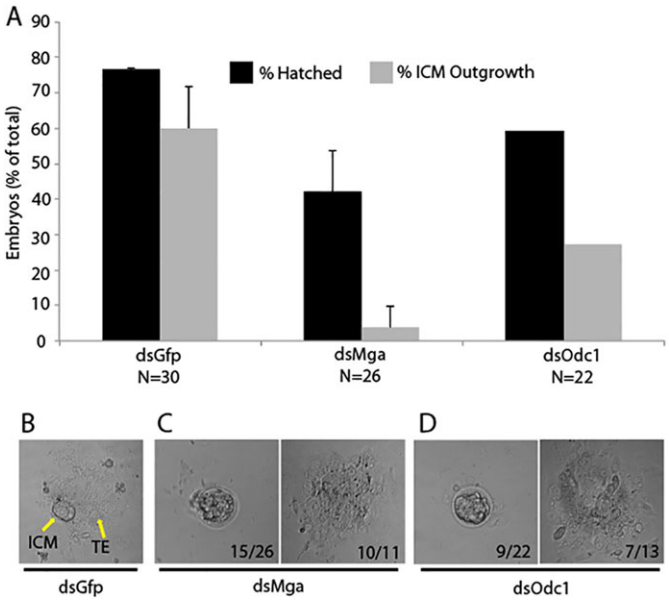

Fig. 4. Knockdown of *Mga* or *Odc1* results in ICM failure. (A) Results of outgrowth assays following injection with dsGfp, dsMga or dsOdc1. All injection groups developed to the blastocyst stage at similar rates (~90%, not shown). Percentage of total embryos (*N*) that hatched and formed ICM outgrowths is shown for each group. (B) Control embryos (dsGfp) form obvious ICM colonies and TE outgrowths (yellow arrows). (C,D) Examples of the failure to hatch and failure to form ICM outgrowth after microinjection of dsMga or dsOdc1. The numbers in the panels refer to the number of embryos out of the total that failed to hatch (as shown) or the number of embryos out of the total that hatched and outgrew that failed to form an ICM (as shown).

Mga. Conversely, the lack of an early effect on GATA4-expressing cells reflects a lack of requirement for *Mga* in initial PE differentiation and in differentiated cells.

Expression of the Myc target gene *ornithine decarboxylase 1* (*Odc1*) is decreased in embryos lacking *Mga*

Based on a similar expression pattern and embryonic mutant phenotype as well as its regulation by the bHLHZip factor MYC (Pendeville et al., 2001), we identified *Odc1*, the gene coding for ornithine decarboxylase (ODC), as a candidate downstream target of MGA. ODC catalyzes the decarboxylation of ornithine to form putrescine, the rate-limiting step in the polyamine synthesis pathway for the production of spermine and spermidine (Fig. 7A).

To assess the function of ODC1 in peri-implantation embryos, we knocked down *Odc1* by microinjection of dsOdc1 double-stranded RNA into one-cell zygotes. dsOdc1 embryos developed normally to the blastocyst stage. Outgrowth assays revealed that, whereas 59% (13/22) of dsOdc1 blastocysts hatched from the zona pellucida and attached to the culture dish, only 27% (6/22) showed evidence of ICM formation (Fig. 4). Similar to $Mga^{Gt/Gt}$ and dsMga embryos, outgrowth of TE cells in dsOdc1 embryos was not different from control dsGFP outgrowths.

To directly assess ODC levels, immunofluorescence was performed with antibodies against ODC. Projections of confocal stacks showed decreased ODC signal in the EPI of $Mga^{Gt/Gt}$ embryos (4/6) at E4.5 compared with $Mga^{+/+}$ and $Mga^{Gt/+}$ embryos (3/31) (P=0.006; Fisher's Exact Probability test) (Fig. 7B). There was also strong fluorescence on the TE in all samples, although secondary antibody controls (data not shown) indicated that this was background staining.

Exogenous putrescine rescues the ICM in *Mga* mutant embryos and survival of *Mga* mutant ESCs

Because decreased *Odc1* expression in $Mga^{Gt/Gt}$ embryos suggests that they lack the ability to produce putrescine and thus lack the end products of the polyamine synthesis pathway, we attempted to rescue $Mga^{Gt/Gt}$embryos by supplying blastocyst cultures with exogenous putrescine and measuring ICM and TE outgrowth area after 96 h. Putrescine did not affect the outgrowth area of TE, but the ICM area of $Mga^{Gt/Gt}$ embryos was significantly larger in embryos treated with putrescine (n=11) than in untreated embryos (n=7) (t=−4.58, P=0.0003), whereas the area of the ICM in $Mga^{+/+}$ and $Mga^{Gt/+}$ embryos was similar with (n=29) or without putrescine (n=24) (t=1.4, P=0.18) (Fig. 7C). Notably, the ICM area of the $Mga^{Gt/Gt}$ cultures was not significantly different than the putrescine-treated control cultures (t=−1.83, P=0.08). These results indicate that exogenous putrescine is sufficient to rescue the ICM outgrowth of $Mga^{Gt/Gt}$ embryos.

To determine whether putrescine could also rescue *Mga* mutant ESCs, $Mga^{Inv/Inv}$; *creERT2* ESCs were plated and allowed to attach for 1 day. Cultures were then supplemented with 4-hydroxytamoxifen, 4-hydroxytamoxifen plus 200 µM putrescine or with putrescine alone. After an additional 2 days of culture, cell counts from $Mga^{Inv/Inv}$; *creERT2* cultures with 4-hydroxytamoxifen plus putrescine were higher than with 4-hydroxytamoxifen alone (t=6.14; P<0.0001), but not as high as untreated $Mga^{Inv/Inv}$; *creERT2* ESCs (t=3.17; P=0.0036). This suggests that $Mga^{Re\text{-}inv/Re\text{-}inv}$; *creERT2* ESC are

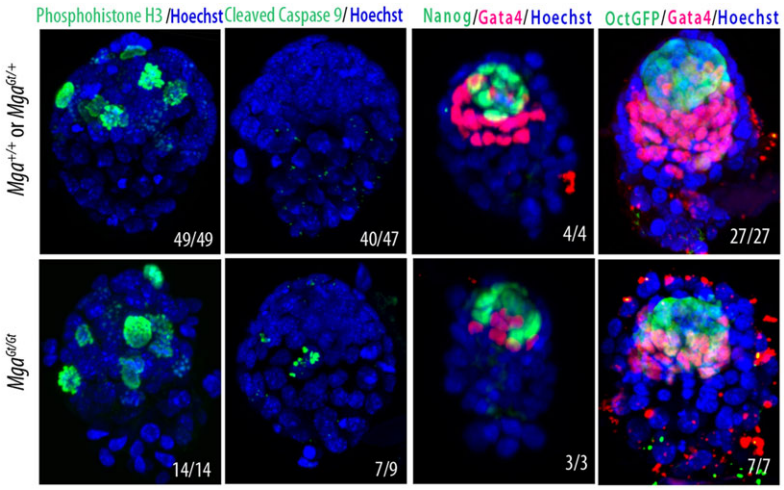

Fig. 5. $Mga^{Gt/Gt}$ embryos showed more apoptosis, but cell proliferation and differentiation were normal at E4.5. Cell proliferation, as measured by phospho-H3 immunostaining, was similar in $Mga^{Gt/Gt}$ compared with $Mga^{+/+}$ and $Mga^{Gt/+}$ embryos. Confocal *Z*-stacks of cleaved caspase 9 immunofluorescence showed that more $Mga^{Gt/Gt}$ embryos had fragmented nuclei (7/9) than did $Mga^{+/+}$ and $Mga^{Gt/+}$ embryos (7/47). The pluripotency markers NANOG and POU5F1, as measured by a GFP reporter, are similar in $Mga^{Gt/Gt}$ embryos compared with $Mga^{+/+}$ and $Mga^{Gt/+}$ embryos, as was the PE marker GATA4. Numbers in the panels indicate the number of embryos out to the total with an appearance similar to that shown.

Development (2015) 142, 31-40 doi:10.1242/dev.111104

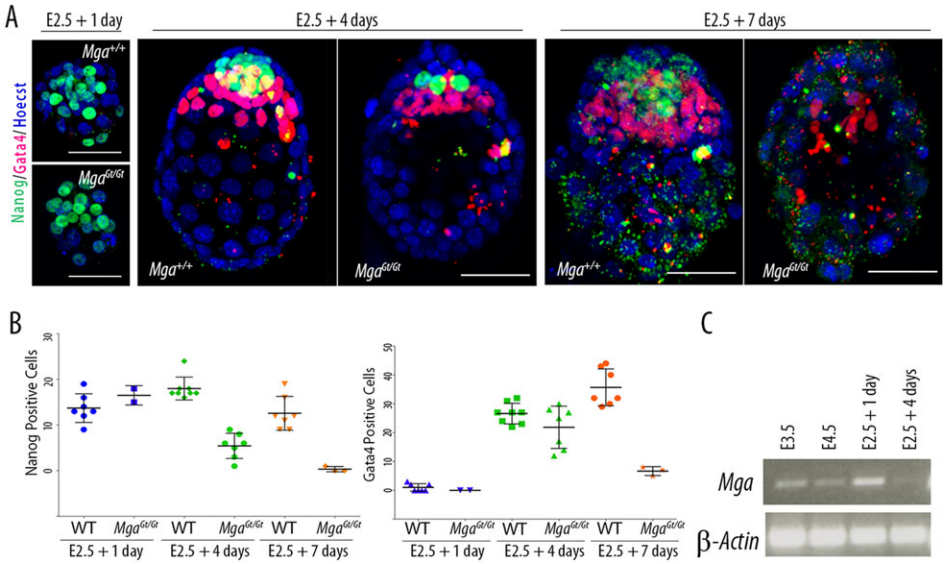

Fig. 6. Pluripotent EPI cells are lost during diapause. (A) Following induction of diapause at E2.5, NANOG-positive cells (green) are gradually lost from $Mga^{Gt/Gt}$ embryos. GATA4-positive cells (red) persist longer but decrease in number by E2.5+7 days. Scale bars: 100 µm. (B) The number of NANOG-positive cells is significantly lower in $Mga^{Gt/Gt}$ embryos at 4 and 7 days of diapause, whereas GATA4-positive cells are significantly different only at 7 days of diapause. WT includes $Mga^{+/+}$ and $Mga^{Gt/+}$ embryos. Each point represents one embryo. (C) RT-PCR indicates that one day after diapause is induced, *Mga* is expressed in wild-type embryos at levels comparable to E3.5 and then declines during diapause.

able to survive but that other factors might be required to completely compensate for the loss of *Mga*. Putrescine alone had no effect. (t=−0.152, *P*=0.88) (Fig. 7C). To test the specificity of putrescine, $Mga^{Inv/Inv}$; *creERT2* cultures were treated with cadaverine, a structurally related cationic polyamine that has an additional carbon link in its backbone but is not part of the polyamine synthesis pathway. Cadaverine treatment had no effect on $Mga^{Inv/Inv}$; *creERT2* cultures alone (t=−0.26, *P*=0.80) or when combined with 4-hydroxytamoxifen (t=0.05, *P*=0.96). None of the supplemented media combinations used had any effect on $Mga^{Inv/+}$ or $Mga^{+/+}$; *creERT2* ESC lines (data not shown).

By culturing $Mga^{Inv/Inv}$; *creERT2* ESCs with 4-hydroxytamoxifen plus putrescine, two $Mga^{Re\text{-}inv/Re\text{-}inv}$; *creERT2* subclones were derived. Both of these lines showed a decrease in the number of cells 48 h after the removal of putrescine (t=3.60, *P*=0.023; t=4.99, *P*=0.001) (Fig. 7C). Linear regression of the cell counts on each day of culture showed decreasing numbers of surviving cells in cultures without exogenous putrescine compared with cultures with putrescine (y=−0.06, R^2=0.74; y=−0.06, R^2=0.69). Immunofluorescence with antibodies against ODC was performed on $Mga^{Re\text{-}inv/Re\text{-}inv}$; *creERT2* ESC lines grown in the presence of exogenous putrescine. Both cell lines showed decreased ODC signal in ESC colonies compared with control $Mga^{Inv/Inv}$; *creERT2* ESCs with or without putrescine. All cell lines showed heterogeneous NANOG staining throughout the ESC colonies (Fig. 7B).

ESCs grown in LIF- and serum-containing medium contain both self-renewing cells and a spectrum of cells in transition toward differentiation, whereas 2i conditions favor a more uniform population of core pluripotent cells in a ground state over cells primed for differentiation (Marks et al., 2012). We grew $Mga^{Re\text{-}inv/Re\text{-}inv}$; *creERT2* ESCs in 2i conditions and tested the effect of exogenous putrescine. Unlike the result for ESCs cultured in mES media, there was no significant difference in cell counts after 48 h with or without putrescine (t=1.82, *P*=0.09) (Fig. 7C). This

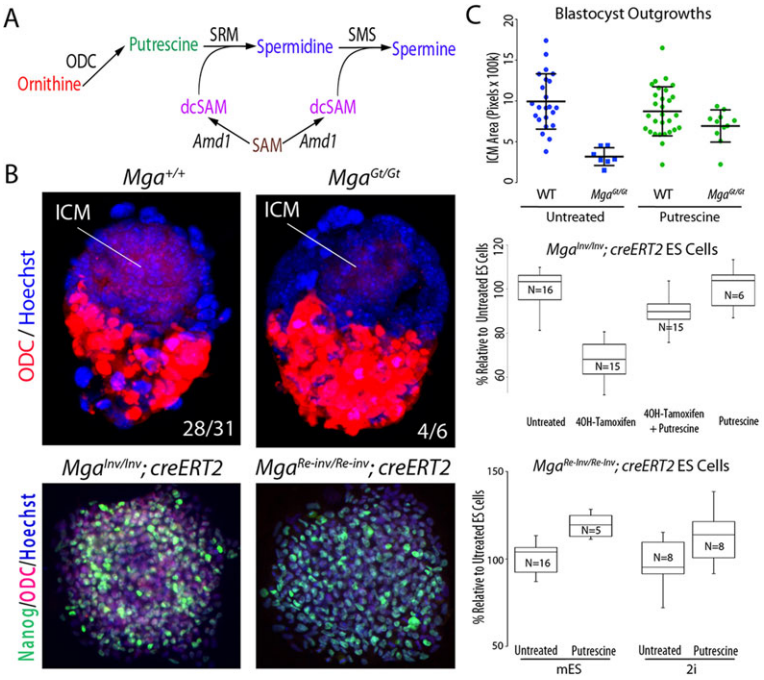

Fig. 7. Polyamine synthesis pathway and the expression of ODC in E4.5 embryos. (A) ODC is the rate-limiting step in the polyamine synthesis pathway that produces spermine and spermidine. ODC catalyzes the conversion of ornithine to putrescine. Putrescine is then converted into spermidine and spermine with the addition of decarboxylated S-adenosyl-methionine (dcSAM). (B) Projections of confocal *Z*-stacks show lower levels of ODC (red) in the EPI of $Mga^{Gt/Gt}$ embryos at E4.5. Secondary antibody background is present on the TE of all embryos tested (top). $Mga^{Re\text{-}inv/Re\text{-}inv}$; *creERT2* ESCs treated with putrescine also show a lower level of ODC (red) compared with $Mga^{Inv/Inv}$; *creERT2* ESCs when treated with putrescine (bottom). Numbers in panels indicate the number of embryos out of the total with an appearance similar to that shown. (C) ICM surface area after 4 days of culture of treated $Mga^{Gt/Gt}$ cultures was greater than of untreated $Mga^{Gt/Gt}$ cultures and was not different from treated $Mga^{+/+}$ or $Mga^{Gt/+}$ cultures (top). Greater numbers of $Mga^{Inv/Inv}$; *creERT2* ESCs that had inversion induced with 4OH-tamoxifen were present after 2 days of culture when treated with putrescine than when treated with 4OH-tamoxifen alone. Putrescine alone had no effect (middle). $Mga^{Re\text{-}inv/Re\text{-}inv}$; *creERT2* ESCs were less affected by exogenous putrescine when cultured in 2i conditions compared with mES conditions (bottom). *N*=number of replicate culture wells.

Development (2015) 142, 31-40 doi:10.1242/dev.111104

indicates that the putrescine-mediated rescue of *Mga*-deficient ESCs, and thus the requirement for ODC, is more marked in the more heterogeneous EPI-like pluripotent cell population favored by mES culture conditions than on the naïve ICM-like pluripotent cells favored by 2i culture conditions.

DISCUSSION

The insertion of a gene trap cassette into the third intron of *Mga* results in a fusion protein containing the T-box and a functional β-galactosidase reporter but lacking the rest of the Mga protein, including the bHLHZip domain. The allele lacks a heterozygous phenotype, indicating that it is not acting as a dominant negative, in spite of the presence of the T-box in the fusion protein. Homozygous $Mga^{Gt/Gt}$ embryos, on the other hand, have a defect in ICM derivatives in which *Mga* transcripts have been detected (Yoshikawa et al., 2006). Moreover, embryos in which Mga was knocked down by RNAi had a blastocyst outgrowth phenotype similar to $Mga^{Gt/Gt}$ embryos. Thus, the gene trap allele Mga^{Gt} appears to be functionally equivalent to a null allele. In addition, the conditional Mga^{Inv} allele, derived from the Mga^{Gt} allele, is not fully functional, as mice homozygous for Mga^{Inv} can survive but are not recovered at Mendelian frequencies, and no $Mga^{Gt/Inv}$ compound heterozygotes were recovered.

Homozygous $Mga^{Gt/Gt}$ embryos implant in the uterus, but ICM derivatives fail to develop beyond E4.5 and show increased apoptosis but no change in cell proliferation. Similarly, *in vitro*, mutant blastocysts attach and TE outgrows, but the ICM fails to survive. ESCs derived using the conditional Mga^{Inv} allele also fail to thrive when the conditional allele is inverted to the $Mga^{Re\text{-}inv}$ configuration. As the expression of *Mga* is restricted to the ICM of embryos at E3.5 and the EPI of later embryos, these results indicate that embryonic lethality is caused by the defective development of the ICM and EPI. The *Mga* mutant phenotype is similar to that of mice mutant for ICM- or EPI-specific genes associated with pluripotency, notably *Pou5f1* and *Sox2* (Avilion et al., 2003; Nichols et al., 1998). However, the EPI of peri-implantation *Mga* mutants does not appear to lose pluripotency, as judged by expression of *Pou5f1* and *Nanog*. Additionally, the differentiation of PE is normal in *Mga* mutant embryos at E4.5, indicating that loss of *Mga* does not affect this early differentiation event within the ICM.

To investigate whether pluripotent cells could be maintained in *Mga* mutant embryos, we challenged the embryos by inducing diapause to delay implantation (Nichols et al., 2001). Strikingly, despite entering diapause with a similar number of pluripotent cells, mutant embryos rapidly lost NANOG-expressing EPI cells during delayed implantation. The number of differentiated, GATA4-positive PE cells, by contrast, was initially similar to wild-type embryos and declined only after prolonged delay. This suggests that the lack of *Mga* primarily affects the maintenance of the pluripotent cells, not the survival of differentiated cells. Death of PE later in diapause could be a secondary effect of the loss of EPI.

Based on phenotypic similarity of the mouse mutants as well as the presence of E-box sites in its promoter (Bello-Fernandez et al., 1993; Pendeville et al., 2001), we identified *Odc1* as a candidate gene responsible for the death of the pluripotent cells of *Mga* mutant embryo. *Odc1* codes for ODC, the rate-limiting enzyme in the synthesis of putrescine from ornithine in the polyamine synthesis pathway (Fig. 7A). Disruption of this pathway *in vitro* and *in vivo* has shown that polyamines have important roles in pluripotency and peri-implantation development. *Odc1* mutant embryos die shortly after implantation, with a phenotype remarkably similar to that of *Mga* mutant embryos, although, unlike *Mga* mutant embryos, their growth *in vitro* is not rescued by exogenous putrescine (Pendeville et al., 2001). On the other hand, mutation of *Amd1*, a rate-limiting enzyme in synthesis of the polyamines spermidine and spermine from putrescine, causes a similar mutant phenotype in which ICM outgrowth *in vitro* is rescued by exogenous spermidine (Nishimura et al., 2002). In ESCs, *Amd1* is essential for self-renewal and is downregulated translationally during differentiation to neural progenitor cells (Zhang et al., 2012a). In F9 teratocarcinoma cells, decreased levels of ODC result in differentiation due to the accumulation of excess decarboxylated S-adenosylmethionine (Frostesjo et al., 1997).

We found that ODC was reduced in the EPI of E4.5 day *Mga* mutant embryos and in *Mga* mutant ESCs. Moreover, we found that culture with exogenous putrescine partially rescued cell survival in both the ICM outgrowths and in ESCs. $Mga^{Re\text{-}inv/Re\text{-}inv}$*; creERT2* ESCs, derived from $Mga^{Inv/Inv}$*; creERT2* ESCs by culturing with tamoxifen and exogenous putrescine, declined dramatically when putrescine was removed from the media. This suggests that a key role of MGA in the peri-implantation development is to regulate the transcription of *Odc1*, and thus the cellular polyamine pool. Although c-MYC is known to directly activate *Odc1* transcription (Bello-Fernandez et al., 1993) in the context of the *Mga* mutant embryo, ODC levels are still decreased, supporting the theory that MGA regulates MYC-MAX target genes *in vivo* (Hurlin et al., 1999). This could come about if, for example, MGA and c-MYC compete for available E-box binding sites (Geerts et al., 2010; Hurlin et al., 1999), or if they compete for available MAX, their obligate heterodimerization partner (Grinberg et al., 2004). Alternately, c-MYC might serve to amplify transcription of *Odc1* after induction of transcription by MGA rather than inducing it on its own. This notion is supported by the fact that, in human colon carcinoma cells and intestinal epithelial cells, *c-Myc* transcription has been shown to be dependent on ODC function, indicating another factor in initial *Odc1* transcription (Celano et al., 1988; Liu et al., 2006). The notion of c-MYC acting as transcriptional amplifier rather than as the transcriptional initiator is supported by the role that c-MYC plays in the global amplification of transcription in ESCs (Lin et al., 2012).

The fact that putrescine does not support full rescue of *Mga* mutant embryos or of ESCs indicates that other targets might be involved. These could be transcriptional targets of Mga or they could be any number of Myc targets for which Mga competes. Mga/Max has also been found complexed with E2f6 in a repression complex involved in gene silencing, which can bind Myc and T-box-binding elements as well as containing chromatin modifiers (Ogawa et al., 2002).

Our results suggest a possible mechanism for *Mga* to play a crucial role in peri-implantation development through interaction with other proteins in the MAX network, notably c-MYC, to regulate transcription of *Odc1*. In the absence of *Mga*, *Odc1* is downregulated, and end products of the polyamine synthesis pathway necessary for the maintenance of the pluripotent cells of the ICM/EPI lineage are not available in sufficient quantities. This regulation of an MYC/MAX target by MGA could also have significance in human cancer, as it has recently been reported that MGA is recurrently inactivated in high-risk chronic lymphocytic leukemia and Richter syndrome, a disease associated with elevated c-Myc levels (De Paoli et al., 2013). Further experiments will provide insight into the mechanism through which disruption of the polyamine pool leads to the loss of pluripotent cell self renewal.

Development (2015) 142, 31-40 doi:10.1242/dev.111104

Table 3. Primer sequences and primer combinations used for genotyping

Primer name	Sequence
AJW360	ATTCCTGTAGGCCCTGGAAG
AJW363	CAGGACAACCTGACACCTCTG
AJW365	CAGCAGATCCATACCCTGCT
AJW236	GGGAGGATTGGGAAGACAAT
AJW366	TTTGAGGGGACGACGACAGTAT
AJW346	CCTCCAGTGCTGGGTGTTAT
AJW349	ACCCTGTTGCCTTCAACATC
AJW371	ATATCGCTGCGCTGGTCGTC
AJW372	AGGATGGCGTGAGGGAGAGC
Genotypes tested	**Primer combination**
$Mga^{+/+}$, $Mga^{Gt/+}$, $Mga^{Gt/Gt}$	AJW360/AJW363/AJW365
$Mga^{Inv/Inv}$, $Mga^{Inv/+}$	AJW360/AJW363/AJW366
$Mga^{Re\text{-}inv/inv}$	AJW360/AJW366/AJW236

However, loss of control of the cell cycle and subsequent apoptosis seems a likely mechanism, based on the oncogenic potential of tissues that have aberrant polyamine pools (Erdman et al., 1999; Scuoppo et al., 2012). It is also possible that apoptosis is driven by DNA instability or reactive oxygen species, based on the role that polyamines have been shown to play in both processes [reviewed by Seiler and Raul (2005)]. Given the myriad roles that polyamines play in cellular homeostasis, it is possible that loss of pluripotency is the final effect of multiple deregulated processes.

MATERIALS AND METHODS

Mice and genotyping

ESC clones were isolated from E14Tg2a ESCs (Sv129P2) after retroviral infection using rsFlpRosaβgeo (FlpRBG; www.genetrap.org). The insertion of FlpRBG in intron 3 of *Mga* was identified by splinkerette PCR (Horn et al., 2007). Mice carrying the $Mga^{Gt(E153E01)Wrst}$ allele were obtained from the German Gene Trap Consortium and crossed with ICR mice (Taconic Farms). The allele and its derivatives are referred to as Mga^{Gt} (for gene trap), Mga^{Inv} (for FLP-recombinase inverted gene trap) and $Mga^{Re\text{-}inv}$ (for CRE-recombinase re-inverted gene trap). Mice, embryos and ESCs were genotyped using PCR. Ear punches or tail tips were digested in PBND lysis buffer [50 mM KCl, 10 mM Tris-HCl (pH 8.3), 2.5 mM $MgCl_2$-$6H_2O$, 0.1 mg/ml gelatin, 0.45% NP4, 0.45% Tween20] with 100 µg/ml proteinase K (Roche, 03115801001). Cultured embryos were lysed in 15 µl of lysis buffer [10 mM Tris (pH 7.5), 10 mM EDTA, 100 mM NaCl, 0.5% sarkosyl (sodium lauroyl sarcosinate), 100 µg/ml proteinase K] at 55°C for 2 h. Genotyping was performed using three-primer PCR designed to amplify wild-type and mutant bands as indicated in Table 3. PCR conditions were: 4 min at 95°C, followed by 32 cycles of 30 s at 95°C, 30 s at 61°C, 40 s at 72°C and 5 min at 72°C, using 2.5 µM dNTPs, 1× PCR Buffer (Denville, CB3702-7), 1 M Betaine (Sigma, B2629), 2.5 µM primers and Taq polymerase for tails or Herculase II polymerase (Agilent, 600675) for cultured embryos. Embryos were generated and collected from timed matings using the day of a vaginal plug as embryonic day (E) 0.5. Use of vertebrate animals for embryo production was approved by the CUMC and University of Massachusetts Institutional Animal Care and Use Committees.

RT-PCR

For RT-PCR of wild-type embryos, 42 E0.5, 26 E2.5, 35 E3.5 and 29 E4.5 embryos were pooled. RNA was isolated using an RNeasy mini kit (Qiagen, 74104), and RT-PCR was performed using a OneStep RT-PCR kit (Qiagen, 210212) and the primers AJW346 and AJW349 for *Mga*, and AJW371 and AJW372 for *β-actin* (Table 3).

β-galactosidase activity assay

Embryos were fixed for 20 min in 4% paraformaldehyde at 4°C and then washed three times in PBS with 0.1% Tween20 (Fisher, BP337-500). For whole-mount staining, embryos were incubated in X-gal staining buffer [1 mg/ml 5-Bromo-4-chloro-3-indolyl β-D-galactopyranoside in dimethyl sulfoxide (Sigma, B4352), 20 mM K_4Fe, 20 mM K_3Fe, 2 mM $MgCl_2$ in PBS] overnight at 37°C, washed three times in PBS with 0.1% Tween and fixed in 4% paraformaldehyde. For cryosectioning, embryos were transferred to 20% sucrose overnight, embedded in O.C.T. Compound (Tissue-Tek, 4583), sectioned at 10-12 µm, fixed in 4% paraformaldehyde for 10 min at 4°C and incubated in X-gal staining buffer overnight at 37°C. Slides were fixed in 4% paraformaldehyde, counterstained with Eosin Y (Sigma, 318906-500ml) and mounted in Permount (Fisher, SP15-500). For greater sensitivity using Salmon-gal (6-Chloro-3-indolyl-β-D-galactopyranoside; Lab Scientific, X668), embryos were fixed, washed twice with S-Gal rinse solution [0.1% sodium deoxycholate, 0.2% IGEPAL CA-630 (Sigma, I8896), 2 mM $MgCl_2$ and 0.1 M phosphate buffer (pH 7.3)] and incubated with 1 mg/ml Salmon-gal and 6 µg/ml NBT (4-Nitro Blue tetrazolium chloride; Sigma, N6876) dissolved in 70% *N*, *N*-dimethylformamide in water at 37°C for one or more days (Sundararajan et al., 2012).

Blastocyst outgrowth *in vitro*

Blastocyst culture was performed as previously described (Bhatnagar et al., 1995). Briefly, embryos were collected by uterine flushing using M2 media (Sigma, M7167-100ml) at E3.5, zona pellucidae were removed by incubation in acidic Tyrode's solution (Sigma, T1788) and embryos were plated on tissue culture dishes in 20 µl drops of ES media [DMEM, 13% FBS (Hyclone, Cat #SH30071.03 Lot #ARG27092), 1% penicillin/streptomycin, 1% GlutaMax, 1% sodium pyruvate, 1% non-essential amino acids, 0.1% β-mercaptoethanol, LIF derived from CHO cells expressing *Lif*] and covered in mineral oil. Some embryos were cultured in ES media for 1-2 days until they had attached and started to outgrow, and were then cultured for two additional days in 2i media (Millipore, ESGRO-2i SF016). For rescue experiments, embryos were cultured in ES media with 200 µM putrescine (Sigma, P5780-5g). Cultures were photographed daily, and the surface area of the ICM and trophoblast was assessed by morphology and/or quantified using ImageJ (NIH). Following culture, embryos were scraped off of the dish and genotyped.

Immunohistochemistry

Immunohistochemistry was performed as previously described (Artus et al., 2010). Embryos were cultured in DMEM/HEPES (Gibco, 12430-054) and 10% FBS (Hyclone, Cat #SH30071.03 Lot #ARG27092) for 20 min at 37°C in 5% CO_2, fixed in 4% paraformaldehyde with 0.1% Tween20 and 0.01% Triton X-100 (Fisher, BP151-500) for 10 min at room temperature or overnight at 4°C, washed in PBT (PBS with 0.1% Triton X-100), permeabilized with 0.5% Triton X-100 for 20 min at room temperature and washed three times with PBT. Antigens were unmasked with NH_4Cl (Sigma, A-4514) in PBT for 10 min at room temperature. Following washes, embryos were blocked in 2% donkey serum in PBT for 45 min at room temperature, incubated with the first primary antibody overnight at 4°C in 2% donkey serum, washed three times with PBT and incubated with the second primary antibody overnight at 4°C in 2% donkey serum. The following day, embryos were washed three times with PBT, incubated with secondary antibody overnight at 4°C in the dark, washed three times with PBT and incubated with Hoechst 33342 (Sigma, B2261) diluted 1:500 overnight at 4°C in the dark. Embryos were analyzed using a Nikon A1R confocal microscope and NIS Elements v4.0 software. Embryos were then lysed and genotyped with Herculase II polymerase. Statistics were analyzed using Fisher's Exact Probability test. Antibodies used were rabbit anti-NANOG (Abcam, ab80892; 1:50), rabbit anti-GFP (Invitrogen, A11122; 1:50), anti-GATA-4 (Santa Cruz Biotechnology, sc1237; 1:100) and anti-ODC1 (Developmental Studies Hybridoma Bank, CPTC-ODC1-1-s; 1:10).

Embryonic diapause

Diapause was induced in pregnant females at E2.5 by subcutaneous injection of 3 mg DMPA suspended in PBS (Medroxyprogesterone

Development (2015) 142, 31-40 doi:10.1242/dev.111104

17-acetate; Sigma, M1629-1g) and intraperitoneal injection of 20 µg tamoxifen in sunflower seed oil (Sigma, T5648-1g). Embryos were flushed from the uterus with M2 1-7 days later.

ESC derivation and culture

Mga$^{Inv/Inv}$*; creERT2* and *Mga*$^{Inv/+}$ ESC lines were derived using established protocols (Batlle-Morera et al., 2008). Briefly, diapause was induced at E2.5, embryos were recovered at E4.5, washed in Ham's F12 media, incubated in 20% rabbit anti-mouse serum antibody (Sigma, M5774) in Ham's F12 for 30 min at 37°C in 7% CO_2 in air. Embryos were then incubated with 20% guinea pig complement (CalBiochem, 234395) in Ham's F12 for immunosurgical isolation of ICMs. ICMs were plated on gelatin-coated tissue culture dishes in mES media supplemented with recombinant human 100 µg/ml BMP4 (R&D Systems, 314-BP-010) and 50 mM MEK inhibitor PD98059 (Cell Signaling Technology, 9900S). After 7-10 days, ICM outgrowths were trypsinized with 0.25% trypsin and replated on mitomycin-C (Sigma, M4287)-treated MEFs. Inversion of the *Mga* allele was induced using 0.5 µM 4-hydroxytamoxifen (Sigma, H6278). Some cultures were supplemented with 200 µM putrescine (Sigma, P5780-5g) or 200 µM cadaverine (Sigma, D22606) dissolved in water. For cell counts, cells were allowed to attach over night and were then treated for 48 h, trypsinized and counted on a hemocytometer. Statistics were analyzed using Student's *t*-test.

RNAi embryo production, microinjection and culture

B6D2F1 female mice were superovulated with 5 IU pregnant mare's serum gonadotropin (PMSG) (Sigma) followed by 5 IU human chorionic gonadotropin (hCG) (Sigma) 48 h later and were mated with B6D2F1 males. Zygotes were collected at 21 h post hCG. Cumulus cells were removed with hyaluronidase (ICN Pharmaceuticals). dsRNA was microinjected into the cytoplasm of zygotes with a Piezo-drill (Prime Tech, Japan) and Eppendorf Transferman micromanipulators. 1 µg/µl dsRNA was loaded into a microinjection pipette and constant flow was adjusted to allow successful microinjection. Approximately 5-10 pl dsRNA was injected into the cytoplasm of each embryo. Zygotes were cultured in KSOM (EmbryoMax, Millipore) at 37°C in 5% CO_2/5% O_2.

Double-stranded RNA (dsRNA) preparation

DNA templates for T7-RNA polymerase-mediated dsRNA production were amplified from genomic DNA or preimplantation embryo cDNA using primers that contained the T7 binding sequences, followed by gene-specific sequences. *In vitro* transcription was performed using T7 MEGAscript Kit (Ambion), and 0.5 µl of TURBO RNase-free DNase was added to each 10-µl reaction to remove the DNA template. dsRNA was treated with NucAway Spin Columns (Ambion) to recover the dsRNA. The dsRNA was then extracted with phenol:chloroform, precipitated with 70% ethanol and resuspended in RNase-free water. The concentration of dsRNA was measured by NanoDrop, diluted to 1 µg/µl and stored at −80°C until use.

Acknowledgements

We thank members of the Papaioannou lab and Drs Michael Shen and Chloe Bulinski for constructive criticism, and Akiko DeSantis for expert technical assistance.

Competing interests

The authors declare no competing financial interests.

Author contributions

W.W. and T.F. designed and produced the gene trap mutation and produced the mutant mice. C.S. helped developing the concept and carried out preliminary experiments. K.Z. and J.M. designed and carried out the dsRNA experiments. A.J.W. and V.E.P. developed the concept, designed and carried out experiments and data analysis, and prepared and edited the manuscript. All authors edited and approved the final manuscript.

Funding

Research reported in this publication was supported by a Kompetenznetz Degenerative Demenzen (KNDD2) grant [FKZ 01 GI 1005D to T.F.], the grant 'Funktionelle Tiermodelle für die Kandidatengene der Alzheimerschen Erkrankung' [01GS08133 to W.W.] from the Federal Ministry for Education and Research (BMBF), the Helmholtz Alliance 'Mental Health in an Ageing Society' (HELMA) [HA215 to W.W.], the European Commission [FP7-HEALTH-F4-2010-261492 to W.W], a March of Dimes Research Grant [#6-FY11-367 to J.M.], and the Eunice Kennedy Shriver National Institute of Child Health & Human Development of the National Institutes of Health (NIH) [R37HD033082 to V.E.P.]. A.J.W. was supported by an NIH Training Grant [GM008798]. The content is solely the responsibility of the authors and does not necessarily represent the official views of the NIH. Deposited in PMC for release after 12 months.

References

Artus, J., Panthier, J.-J. and Hadjantonakis, A.-K. (2010). A role for PDGF signaling in expansion of the extra-embryonic endoderm lineage of the mouse blastocyst. *Development* **137**, 3361-3372.

Avilion, A. A., Nicolis, S. K., Pevny, L. H., Perez, L., Vivian, N. and Lovell-Badge, R. (2003). Multipotent cell lineages in early mouse development depend on SOX2 function. *Genes Dev.* **17**, 126-140.

Ayer, D. E., Kretzner, L. and Eisenman, R. N. (1993). Mad: a heterodimeric partner for Max that antagonizes Myc transcriptional activity. *Cell* **72**, 211-222.

Batlle-Morera, L., Smith, A. and Nichols, J. (2008). Parameters influencing derivation of embryonic stem cells from murine embryos. *Genesis* **46**, 758-767.

Baudino, T. A. and Cleveland, J. L. (2001). The Max network gone mad. *Mol. Cell. Biol.* **21**, 691-702.

Bello-Fernandez, C., Packham, G. and Cleveland, J. L. (1993). The ornithine decarboxylase gene is a transcriptional target of c-Myc. *Proc. Natl. Acad. Sci. USA* **90**, 7804-7808.

Bhatnagar, P., Papaioannou, V. E. and Biggers, J. D. (1995). CSF-1 and mouse preimplantation development in vitro. *Development* **121**, 1333-1339.

Brenner, R. M., Slayden, O. D., Rodgers, W. H., Critchley, H. O. D., Carroll, R., Jing Nie, X. and Mah, K. (2003). Immunocytochemical assessment of mitotic activity with an antibody to phosphorylated histone H3 in the macaque and human endometrium. *Hum. Reprod.* **18**, 1185-1193.

Celano, P., Baylin, S. B., Giardiello, F. M., Nelkin, B. D. and Casero, R. A.Jr,. (1988). Effect of polyamine depletion on c-myc expression in human colon carcinoma cells. *J. Biol. Chem.* **263**, 5491-5494.

Chazaud, C., Yamanaka, Y., Pawson, T. and Rossant, J. (2006). Early lineage segregation between epiblast and primitive endoderm in mouse blastocysts through the Grb2-MAPK pathway. *Dev. Cell* **10**, 615-624.

de Luca, C., Kowalski, T. J., Zhang, Y., Elmquist, J. K., Lee, C., Kilimann, M. W., Ludwig, T., Liu, S.-M. and Chua, S. C.Jr,. (2005). Complete rescue of obesity, diabetes, and infertility in db/db mice by neuron-specific LEPR-B transgenes. *J. Clin. Invest.* **115**, 3484-3493.

De Paoli, L., Cerri, M., Monti, S., Rasi, S., Spina, V., Bruscaggin, A., Greco, M., Ciardullo, C., Famà, R., Cresta, S. et al. (2013). MGA, a suppressor of MYC, is recurrently inactivated in high risk chronic lymphocytic leukemia. *Leuk. Lymphoma* **54**, 1087-1090.

Erdman, S. H., Ignatenko, N. A., Powell, M. B., Blohm-Mangone, K. A., Holubec, H., Guillen-Rodriguez, J. M. and Gerner, E. W. (1999). APC-dependent changes in expression of genes influencing polyamine metabolism, and consequences for gastrointestinal carcinogenesis, in the Min mouse. *Carcinogenesis* **20**, 1709-1713.

Frostesjo, L., Holm, I., Grahn, B., Page, A. W., Bestor, T. H. and Heby, O. (1997). Interference with DNA methyltransferase activity and genome methylation during F9 teratocarcinoma stem cell differentiation induced by polyamine depletion. *J. Biol. Chem.* **272**, 4359-4366.

Geerts, D., Koster, J., Albert, D., Koomoa, D.-L. T., Feith, D. J., Pegg, A. E., Volckmann, R., Caron, H., Versteeg, R. and Bachmann, A. S. (2010). The polyamine metabolism genes ornithine decarboxylase and antizyme 2 predict aggressive behavior in neuroblastomas with and without MYCN amplification. *Int. J. Cancer* **126**, 2012-2024.

Grandori, C., Cowley, S. M., James, L. P. and Eisenman, R. N. (2000). The Myc/Max/Mad network and the transcriptional control of cell behavior. *Annu. Rev. Cell Dev. Biol.* **16**, 653-699.

Grinberg, A. V., Hu, C.-D. and Kerppola, T. K. (2004). Visualization of Myc/Max/Mad family dimers and the competition for dimerization in living cells. *Mol. Cell. Biol.* **24**, 4294-4308.

Hammachi, F., Morrison, G. M., Sharov, A. A., Livigni, A., Narayan, S., Papapetrou, E. P., O'Malley, J., Kaji, K., Ko, M. S. H., Ptashne, M. et al. (2012). Transcriptional activation by Oct4 is sufficient for the maintenance and induction of pluripotency. *Cell Rep.* **1**, 99-109.

Horn, C., Hansen, J., Schnütgen, F., Seisenberger, C., Floss, T., Irgang, M., De-Zolt, S., Wurst, W., von Melchner, H. and Noppinger, P. R. (2007). Splinkerette PCR for more efficient characterization of gene trap events. *Nat. Genet.* **39**, 933-934.

Hu, G., Kim, J., Xu, Q., Leng, Y., Orkin, S. H. and Elledge, S. J. (2009). A genome-wide RNAi screen identifies a new transcriptional module required for self-renewal. *Genes Dev.* **23**, 837-848.

Hurlin, P. J. and Huang, J. (2006). The MAX-interacting transcription factor network. *Semin. Cancer Biol.* **16**, 265-274.
Hurlin, P. J., Queva, C., Koskinen, P. J., Steingrimsson, E., Ayer, D. E., Copeland, N. G., Jenkins, N. A. and Eisenman, R. N. (1995). Mad3 and Mad4: novel Max-interacting transcriptional repressors that suppress c-myc dependent transformation and are expressed during neural and epidermal differentiation. *EMBO J.* **14**, 5646-5659.
Hurlin, P. J., Steingrìmsson, E., Copeland, N. G., Jenkins, N. A. and Eisenman, R. N. (1999). Mga, a dual-specificity transcription factor that interacts with Max and contains a T-domain DNA-binding motif. *EMBO J.* **18**, 7019-7028.
Jedrusik, A., Parfitt, D.-E., Guo, G., Skamagki, M., Grabarek, J. B., Johnson, M. H., Robson, P. and Zernicka-Goetz, M. (2008). Role of Cdx2 and cell polarity in cell allocation and specification of trophectoderm and inner cell mass in the mouse embryo. *Genes Dev.* **22**, 2692-2706.
Johnson, M. H. and McConnell, J. M. L. (2004). Lineage allocation and cell polarity during mouse embryogenesis. *Semin. Cell Dev. Biol.* **15**, 583-597.
Lengner, C. J., Camargo, F. D., Hochedlinger, K., Welstead, G. G., Zaidi, S., Gokhale, S., Scholer, H. R., Tomilin, A. and Jaenisch, R. (2007). Oct4 expression is not required for mouse somatic stem cell self-renewal. *Cell Stem Cell* **1**, 403-415.
Lin, C. Y., Lovén, J., Rahl, P. B., Paranal, R. M., Burge, C. B., Bradner, J. E., Lee, T. I. and Young, R. A. (2012). Transcriptional amplification in tumor cells with elevated c-Myc. *Cell* **151**, 56-67.
Liu, L., Guo, X., Rao, J. N., Zou, T., Marasa, B. S., Chen, J., Greenspon, J., Casero, R. A.Jr, and Wang, J.-Y. (2006). Polyamine-modulated c-Myc expression in normal intestinal epithelial cells regulates p21Cip1 transcription through a proximal promoter region. *Biochem. J.* **398**, 257-267.
Loh, Y.-H., Wu, Q., Chew, J.-L., Vega, V. B., Zhang, W., Chen, X., Bourque, G., George, J., Leong, B., Liu, J. et al. (2006). The Oct4 and Nanog transcription network regulates pluripotency in mouse embryonic stem cells. *Nat. Genet.* **38**, 431-440.
Marks, H., Kalkan, T., Menafra, R., Denissov, S., Jones, K., Hofemeister, H., Nichols, J., Kranz, A., Stewart, A. F., Smith, A. et al. (2012). The transcriptional and epigenomic foundations of ground state pluripotency. *Cell* **149**, 590-604.
Meroni, G., Reymond, A., Alcalay, M., Borsani, G., Tanigami, A., Tonlorenzi, R., Lo Nigro, C., Messali, S., Zollo, M., Ledbetter, D. H. et al. (1997). Rox, a novel bHLHZip protein expressed in quiescent cells that heterodimerizes with Max, binds a non-canonical E box and acts as a transcriptional repressor. *EMBO J.* **16**, 2892-2906.
Meroni, G., Cairo, S., Merla, G., Messali, S., Brent, R., Ballabio, A. and Reymond, A. (2000). Mlx, a new Max-like bHLHZip family member: the center stage of a novel transcription factors regulatory pathway? *Oncogene* **19**, 3266-3277.
Nichols, J., Zevnik, B., Anastassiadis, K., Niwa, H., Klewe-Nebenius, D., Chambers, I., Schöler, H. and Smith, A. (1998). Formation of pluripotent stem cells in the mammalian embryo depends on the POU transcription factor Oct4. *Cell* **95**, 379-391.
Nichols, J., Chambers, I., Taga, T. and Smith, A. (2001). Physiological rationale for responsiveness of mouse embryonic stem cells to gp130 cytokines. *Development* **128**, 2333-2339.
Nishimura, K., Nakatsu, F., Kashiwagi, K., Ohno, H., Saito, T. and Igarashi, K. (2002). Essential role of S-adenosylmethionine decarboxylase in mouse embryonic development. *Genes Cells* **7**, 41-47.
Ogawa, H., Ishiguro, K.-i., Gaubatz, S., Livingston, D. M. and Nakatani, Y. (2002). A complex with chromatin modifiers that occupies E2F- and Myc-responsive genes in G_0 Cells. *Science* **296**, 1132-1136.
Pendeville, H., Carpino, N., Marine, J.-C., Takahashi, Y., Muller, M., Martial, J. A. and Cleveland, J. L. (2001). The ornithine decarboxylase gene is essential for cell survival during early murine development. *Mol. Cell. Biol.* **21**, 6549-6558.
Rikin, A. and Evans, T. (2010). The tbx/bHLH transcription factor mga regulates gata4 and organogenesis. *Dev. Dyn.* **239**, 535-547.
Schnutgen, F., De-Zolt, S., Van Sloun, P., Hollatz, M., Floss, T., Hansen, J., Altschmied, J., Seisenberger, C., Ghyselinck, N. B., Ruiz, P. et al. (2005). Genomewide production of multipurpose alleles for the functional analysis of the mouse genome. *Proc. Natl. Acad. Sci. USA* **102**, 7221-7226.
Scuoppo, C., Miething, C., Lindqvist, L., Reyes, J., Ruse, C., Appelmann, I., Yoon, S., Krasnitz, A., Teruya-Feldstein, J., Pappin, D. et al. (2012). A tumour suppressor network relying on the polyamine-hypusine axis. *Nature* **487**, 244-248.
Seiler, N. and Raul, F. (2005). Polyamines and apoptosis. *J. Cell Mol. Med.* **9**, 623-642.
Shen-Li, H., O'Hagan, R., Hou, H., Jr, Horner, J. W., II, Lee, H.-W. and DePinho, R. (2000). Essential role for Max in early embryonic growth and development. *Genes Dev.* **14**, 17-22.
Silva, J., Nichols, J., Theunissen, T. W., Guo, G., van Oosten, A. L., Barrandon, O., Wray, J., Yamanaka, S., Chambers, I. and Smith, A. (2009). Nanog is the gateway to the pluripotent ground state. *Cell* **138**, 722-737.
Strumpf, D., Mao, C.-A., Yamanaka, Y., Ralston, A., Chawengsaksophak, K., Beck, F. and Rossant, J. (2005). Cdx2 is required for correct cell fate specification and differentiation of trophectoderm in the mouse blastocyst. *Development* **132**, 2093-2102.
Sundararajan, S., Wakamiya, M., Behringer, R. R. and Rivera-Perez, J. A. (2012). A fast and sensitive alternative for β-galactosidase detection in mouse embryos. *Development* **139**, 4484-4490.
van den Berg, D. L. C., Snoek, T., Mullin, N. P., Yates, A., Bezstarosti, K., Demmers, J., Chambers, I. and Poot, R. A. (2010). An Oct4-centered protein interaction network in embryonic stem cells. *Cell Stem Cell* **6**, 369-381.
Walker, W., Zhou, Z.-Q., Ota, S., Wynshaw-Boris, A. and Hurlin, P. J. (2005). Mnt-Max to Myc-Max complex switching regulates cell cycle entry. *J. Cell Biol.* **169**, 405-413.
Wianny, F. and Zernicka-Goetz, M. (2000). Specific interference with gene function by double-stranded RNA in early mouse development. *Nat. Cell Biol.* **2**, 70-75.
Yoshikawa, T., Piao, Y., Zhong, J., Matoba, R., Carter, M. G., Wang, Y., Goldberg, I. and Ko, M. S. H. (2006). High-throughput screen for genes predominantly expressed in the ICM of mouse blastocysts by whole mount in situ hybridization. *Gene Expr. Patterns* **6**, 213-224.
Zervos, A. S., Gyuris, J. and Brent, R. (1993). Mxi1, a protein that specifically interacts with Max to bind Myc-Max recognition sites. *Cell* **72**, 223-232.
Zhang, D., Zhao, T., Ang, H. S., Chong, P., Saiki, R., Igarashi, K., Yang, H. and Vardy, L. A. (2012a). AMD1 is essential for ESC self-renewal and is translationally down-regulated on differentiation to neural precursor cells. *Genes Dev.* **26**, 461-473.
Zhang, Z., Theurkauf, W. E., Weng, Z. and Zamore, P. D. (2012b). Strand-specific libraries for high throughput RNA sequencing (RNA-Seq) prepared without poly (A) selection. *Silence* **3**, 9.
Zhu, Q., Jin, L., Casero, R. A., Davidson, N. E. and Huang, Y. (2012). Role of ornithine decarboxylase in regulation of estrogen receptor alpha expression and growth in human breast cancer cells. *Breast Cancer Res. Treat.* **136**, 57-66.